Inductor Design Methods with Low-permeability RF Core Materials

Yehui Han, *Member, IEEE,* and David J. Perreault, *Senior Member, IEEE*

***Abstract*—This paper presents a design procedure for inductors based on low-permeability magnetic materials, for use in very high frequency (VHF) power conversion. The proposed procedure offers an easy and fast way to compare different magnetic materials based on Steinmetz parameters and quickly select the best among them, to estimate the achievable inductor quality factor and size, and to design the inductor. Approximations used in the proposed methods are discussed. Geometry optimization of magnetic-core inductors is also investigated. The proposed design procedure and methods are verified by experiments.**

I. Background

There is a growing interest in switched-mode power electronics capable of efficient operation at very high switching frequencies (e.g., 10-100 MHz) [1]. Power electronics operating at such frequencies include resonant inverters [2]–[11] (e.g., for heating, plasma generation, imaging, and communications) and resonant dc-dc converters [2], [4], [12]–[21] (which utilize high frequency operation to achieve small size and fast transient response.) These designs utilize magnetic components operating at high frequencies, and often under large flux swings. These magnetic components should have a high quality factor to achieve high efficiency power conversion. Unfortunately, most high-permeability magnetic materials exhibit unacceptably high losses at frequencies above a few megahertz. There are some low-permeability materials (e.g., relative permeabilities in the range of 4-40) that can be used effectively at moderate flux swings at frequencies up to many tens of megahertz [22]–[24]. However, working with such low-permeability materials - and the ungapped core structures they are typically available in - presents somewhat different constraints and challenges than with typical high-permeability low-frequency materials [25]. Because of VHF operation and the low-permeability characteristics of such materials, the operating flux density is limited by core loss rather than saturation, and a gap is not necessary to prevent the core from saturating in many applications. Without a gap, the core loss begins to dominate the total loss and copper loss can be ignored in many cases. The performance of a VHF magnetic-core inductor thus depends heavily on the loss characteristics of the magnetic material. Moreover, there appears to be a lack of good design procedures for a selecting among low-permeability magnetic materials and available core sizes.

Y. Han is with the University of Wisconsin-Madison, 2559C Engineering Hall, 1415 Engineering Drive, Madison, WI 53706, USA (email: yehui@engr.wisc.edu).

D. J. Perreault is with the Laboratory for Electromagnetic and Electronic Systems, Massachusetts Institute of Technology, Cambridge, MA 02139, USA (e-mail: djperrea@mit.edu).

This paper, which expands upon an earlier conference paper [26], investigates a design procedure for inductors using low-permeability magnetic materials. This method is based on knowledge of the material loss characteristics, such as collected in [22], [24], and is particularly suited for VHF inductor designs. With the methods developed here, different magnetic materials are compared fairly and conveniently, and both the achievable quality factor and size of a magnetic-core inductor can be evaluated before the final design.

Section II of the paper introduces the inductor design considerations and questions to be addressed. Section III illustrates the inductor design procedure and methods employed in it. Section IV shows some experimental results to verify the design procedure. Section V concludes the paper. In Appendices A and B, we check an important assumption behind our methods as well as investigate geometry optimization problems of magnetic-core inductors.

II. Inductor Design Considerations and Questions

In this paper, we only consider inductor designs under a limited set of conditions in order to make the problem tractable. Nevertheless, these conditions are both very reasonable and practical for inductors at very high frequencies. The limited conditions we address are as follows:

1) Use of ungapped cores made of low-permeability materials.
2) Single-layer, foil wound designs in the skin depth limit on toroidal core shapes. A toroidal inductor design keeps most of flux inside the core, thus reducing EMI/EMC problems. A foil winding design can further reduce the copper loss compared to a wire-wound one [27].
3) Design based on knowledge of Steinmetz parameters for materials of interest. Such parameters are often not published or readily available for these materials, but can be obtained using methods such as that of [22], [24], [28].
4) Design assuming sinusoidal excitation at one frequency. In VHF resonant inverters or converters, inductors often have approximately sinusoidal current at a single frequency. Note that consideration of variable frequency operation, dc currents, and multiple frequency components greatly increases complexity of both loss calculation and design [29]–[34].

Fig. 1 shows an inductor has been designed and fabricated under the above conditions and replaced the original coreless resonant inductor L_s in a 30 MHz Φ_2 inverter [3], [23], [24]. The magnetic-core inductor provides a substantial volumetric advantage over that achievable with a coreless design in this application [23], [24].

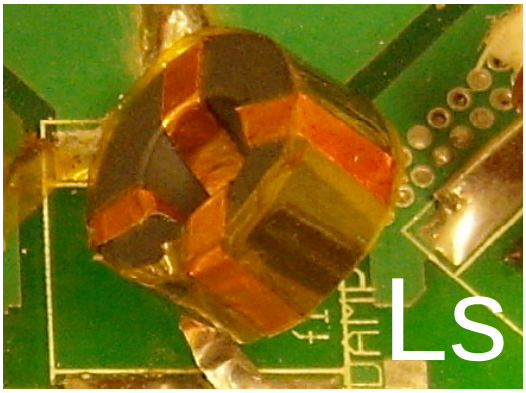

(a) An example of an inductor fabricated from copper foil and a commercial magnetic core of N40 from Ceramic Magnetics.

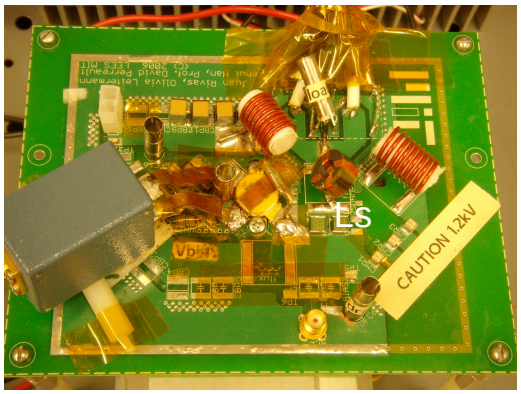

(b) Φ2 inverter with the magnetic-core inductor L_S

Fig. 1. Photographs of the Φ2 inverter prototype with a magnetic-core inductor [24].

Given a selection of available cores in different low-permeability materials, and a design specification including inductance L, current amplitude I_{pk}, frequency f_s, we answer three important questions about design of VHF inductors under the above conditions:

1) Which magnetic material from an available set will yield maximum quality factor Q_L for a given size?
2) Given the ability to continuously scale core size, what material will yield the smallest size for a given quality factor Q_L?
3) For an achievable quality factor Q_L and inductor size, how should we design the inductor with the selected best magnetic material to meet design specifications?

These questions are addressed in the next section.

III. Inductor Design Procedure and Methods

A. Inductor Design Procedure

Fig. 2 provides a high-level illustration of the proposed design procedure. First, select design specifications from the system requirements. Second, select the best magnetic material from a set of low-permeability materials with known Steinmetz parameters. In the third and fourth steps, we estimate the achievable quality factor Q_L and size of the inductor with the best available material. If the results are satisfactory, we design

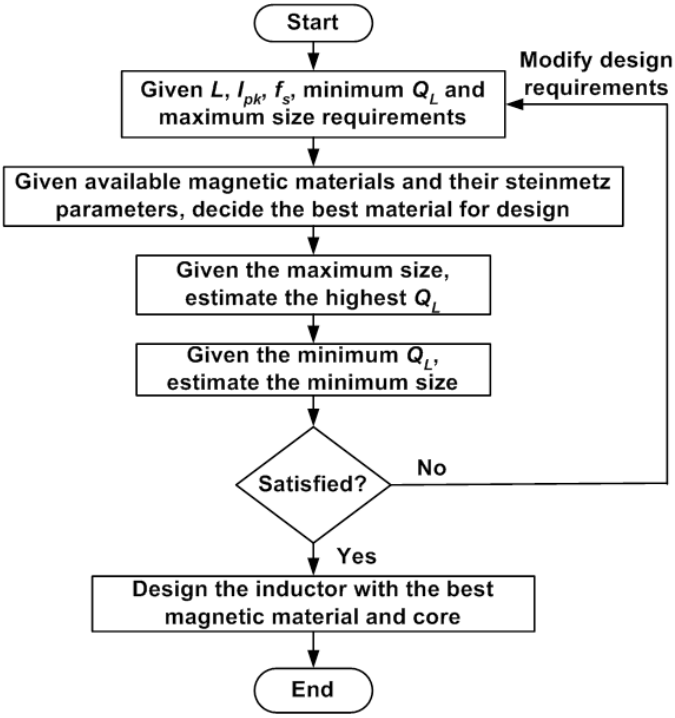

Fig. 2. Inductor design procedure

the inductor. If not, it means the design requirements can't be satisfied even with the best available magnetic material, and one must revise the inductor design requirements. A key feature of this design procedure is that magnetic materials are compared first and the best material is selected before completing any individual design, greatly reducing design time and effort. Some important information such as the maximum quality factor Q_L, and the smallest possible size can be acquired before the final design. By this procedure, we design an inductor only with one size and one material instead of investigating numerous (perhaps thousands) of combinations to meet the design specifications.

(1) to (3) are used often in our design procedure. In VHF power conversion, ac losses (conductor/copper and core losses) usually dominate and we thus ignore dc losses (conductor loss) here. In (1) and (2), we use the quality factor Q_L to evaluate the ac losses of an inductor at a single frequency. R_{ac} is the equivalent total ac resistance of a magnetic-core inductor including copper loss and core loss, R_{cu} is the equivalent resistance owing to copper loss, and R_{co} is an equivalent resistance owing to core loss. The Steinmetz equation is an empirical means to estimate loss characteristics of magnetic materials [35], [36]. It has many extensions [29]–[34], [36]–[38], but we only consider the formulation for sinusoidal drive at a single frequency here. In (3), B_{pk} is the peak amplitude of average (sinusoidal) flux density inside the material and P_V is power loss per unit core volume [1]. K and β are called Steinmetz parameters. K and β have been calculated

[1]Use of average flux density in the core simplifies the calculations. For typical core sizes, this approximation is well justified, and the error of this approximation should be lower than 10% as shown in Appendix A. (Flux nonuniformity for other cases is treated in [39], [40], for example.)

for several commercial low-permeability rf magnetic materials from 20 MHz to 70 MHz in [22], [24], [28].

$$Q_L = \frac{\omega L}{R_{ac}} \tag{1}$$

$$R_{ac} = R_{cu} + R_{co} \tag{2}$$

$$P_V = K B_{pk}^{\beta} \tag{3}$$

B. Method to Select Among Magnetic Materials

In the second step of the design procedure, we identify the best material. We begin with a coreless inductor to make a comparison among different design options (including magnetic materials) for a given L, I_{pk}, f_s, minimum Q_L and maximum size limitation. Ignoring the "single-turn" inductance associated with the circumferential current component around the core [27], the number of turns N_{air} for a coreless inductor can be calculated from (4) [27]:

$$N_{air} \approx \sqrt{\frac{2\pi L}{h\mu_0 \ln\left(\frac{d_o}{d_i}\right)}} \tag{4}$$

d_o, d_i and h are the outside diameter, inside diameter and height of the coreless inductor. The approximate average flux density B_{pk-air} inside the core is calculated by (5):

$$B_{pk-air} = \frac{\mu_0 N_{air} I_{pk}}{0.5\pi(d_i + d_o)} \tag{5}$$

Likewise, the number of turns N and average flux density B_{pk} of a magnetic-core inductor are calculated by (6) and (7) [2]:

$$N \approx \sqrt{\frac{2\pi L}{h\mu_0\mu_r \ln\left(\frac{d_o}{d_i}\right)}} \tag{6}$$

$$B_{pk} = \frac{\mu_0\mu_r N I_{pk}}{0.5\pi(d_i + d_o)} = \mu_r^{0.5} B_{pk-air} \tag{7}$$

For a given L and specified dimensions in (7), average flux density B_{pk} inside the core may be different for each magnetic material, which is one of the reasons we can't compare their loss characteristics for different magnetic materials directly at the same flux density level. However, we propose here a method by which direct comparisons can be made: B_{pk} of each magnetic material can be normalized to the coreless inductor flux density B_{pk-air} by its relative permeability μ_r. For a given design specification, all magnetic materials will have the same normalized flux density, which is equal to $\mu_r^{-0.5} B_{pk}$. Given a set of Steinmetz parameters, we can draw the curves of P_V vs. $\mu_r^{-0.5} B_{pk}$ for all available magnetic materials. We compare P_V of these materials at $\mu_r^{-0.5} B_{pk} = B_{pk-air}$ and decide which material has the smallest core loss for the given design specification.

An example is shown in Fig. 3, in which we consider a design of a magnetic-core inductor at $I_{pk} = 2$ A and

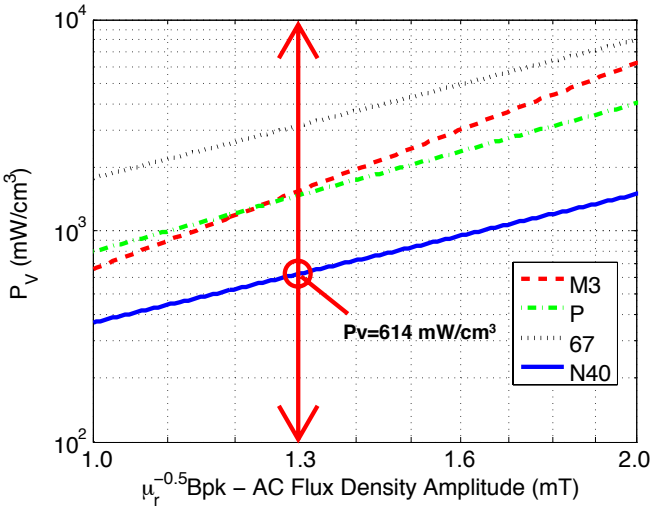

Fig. 3. Inductor design example ($d_o = 12.7$ mm, $d_i = 6.3$ mm, $h = 6.3$ mm, $L = 200$ nH, $I_{pk} = 2$ A, $f_s = 30$ MHz and $B_{pk-air} = 1.3$ mT).

$f_s = 30$ MHz with $L = 200$ nH and maximum size $d_o = 12.7$ mm, $d_i = 6.3$ mm and $h = 6.3$ mm [3]. Beginning with a coreless inductor, we calculate $B_{pk-air} = 1.3$ mT from (4) and (5). Using data from [22], [24], loss curves of P_V vs. $\mu_r^{-0.5} B_{pk}$ are plotted for the materials N40, P, M3 and 67 [4]. We compare their P_V at B_{pk-air} and find that N40 material has the smallest core loss (614 mw/cm^3). If we ignore the copper loss, the magnetic-core inductor with N40 material will achieve the highest Q_L for given design specifications. We can also observe in Fig. 3 that N40 is better than the other magnetic materials and 67 is worse than the others over a wide range of flux density. This will help us to design a magnetic-core inductor if its operating current level is unknown or very wide.

So far, we still don't know if the magnetic-core inductor with the best material is better than a coreless inductor of the same size. There is no core loss and Steinmetz parameters for a coreless inductor. But we can still compare its copper loss to core losses of other magnetic materials on the same graph. To accommodate the coreless design, we define P_{V-air} at B_{pk-air} as the power loss per unit volume for a coreless inductor and calculate it by (8):

$$P_{V-air} = \frac{R_{cu-air}}{2V} I_{pk}^2 \tag{8}$$

R_{cu-air} is the copper resistance of a coreless inductor and V is the volume of the coreless inductor. R_{cu-air} (or the copper resistance of a magnetic-core inductor R_{cu}) depends heavily on a coreless or magnetic-core inductor winding design pattern. One could find the ac resistance of a coreless inductor by constructing and measuring it or simulating it

[2]The relative permeability can be also addressed in a complex form which is equal to $\mu_r' - \mu_r'' j$. μ_r' is equal to μ_r in (6) and (7) and μ_r'' represents the loss which is also a function of flux density. μ_r'' can be calculated from the core loss measurement results in [24]. In this paper, we use curves and Steinmetz parameters to represent losses instead of complex permeability.

[3]Examples in the paper are confined to 30MHz. However, the same design procedure can be applied to a broader range of frequencies.

[4]-17 material in [22], [24] has a very low relative permeability and low core loss characteristics. Compared to its core loss, the copper loss of -17 material can't be ignored. As a special case, -17 is not considered here. However, the methods introduced in this paper can still be applied for -17 material with special considerations of its copper loss.

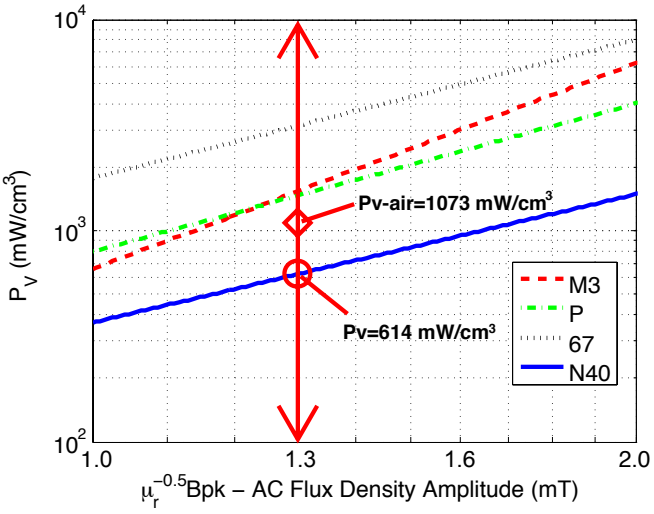

Fig. 4. Inductor design example including the power loss characteristic of a coreless inductor ($d_o = 12.7$ mm, $d_i = 6.3$ mm, $h = 6.3$ mm, $L = 200$ nH, $I_{pk} = 2$ A, $f_s = 30$ MHz and $B_{pk-air} = 1.3$ mT).

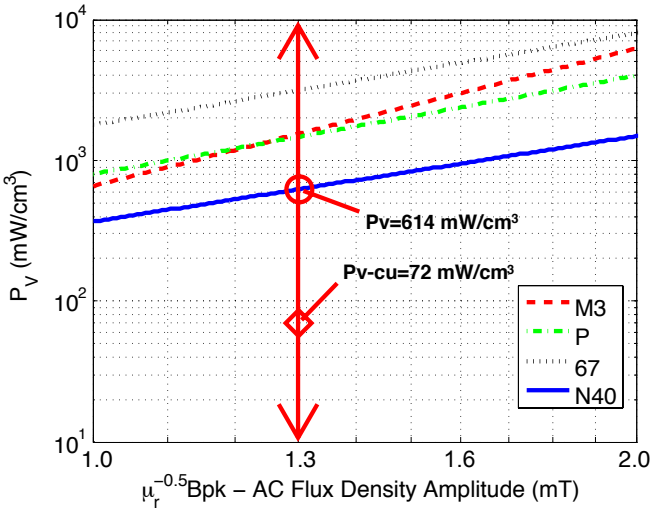

Fig. 5. Inductor design example including the copper loss characteristic of a magnetic-core inductor ($d_o = 12.7$ mm, $d_i = 6.3$ mm, $h = 6.3$ mm, $L = 200$ nH, $I_{pk} = 2$ A, $f_s = 30$ MHz and $B_{pk-air} = 1.3$ mT).

using computational techniques. Alternatively, the resistance can be estimated for different design variants:

1) In [22], [24], the windings are made of an equal-width foil-like conductor, and $R_{cu-single-turn}$ is the ac copper resistance of a single turn inductor:

$$R_{cu} = N^2 R_{cu-single-turn} \approx N^2 \frac{\rho_{cu}}{\pi \delta_{cu}} \left(\frac{2h}{d_i} + \frac{d_o}{d_i} - 1 \right) \quad (9)$$

2) In [22], [24], R_{cu} can alternatively be estimated from the foil width, length and skin depth:

$$R_{cu} \approx \frac{\rho_{cu} l_{cu}}{\delta_{cu} w_{cu}} \quad (10)$$

3) In [27], the windings are made of foil-like conductor tapered to conform to the shape of the toroid:

$$R_{cu} = N^2 R_{cu-single-turn} \approx N^2 \frac{\rho_{cu}}{\pi \delta_{cu}} \left(\frac{h}{d_i} + \frac{h}{d_o} + 2 \ln \frac{d_o}{d_i} \right) \quad (11)$$

For example, the loss characteristics of a coreless inductor estimated by (9) is included in Fig. 4 . We can see N40 is the only magnetic material which has lower loss than the coreless inductor. Thus the magnetic-core inductor built with N40 may have a higher quality factor Q_L than the coreless inductor. The magnetic-core inductor built with other materials (e.g. M3, P and 67) will not be better than the coreless inductor and need not be considered in the following steps. Here, we can see that this comparison lets us exclude most of available magnetic materials in the pool from the design, saving time and effort.

From previous measurements in [22], [24], the core loss (R_{co}) usually dominates the total loss of an ungapped VHF magnetic-core inductor. However, this statement should be checked to make sure that it is still correct for an individual design. By a similar method, we can define the copper loss per unit volume P_{V-cu} of a magnetic-core inductor and mark it on the graph of P_V vs. $\mu_r^{-0.5} B_{pk}$. From (4) and (6),

$$N = \mu_r^{-0.5} N_{air} \quad (12)$$

$$R_{cu} = N^2 R_{cu-single-turn} = \mu_r^{-1} R_{cu-air} \quad (13)$$

$$P_{V-cu} = \frac{R_{cu}}{2V} I_{pk}^2 = \frac{\mu_r^{-1} R_{cu-air}}{2V} I_{pk}^2 = \mu_r^{-1} P_{V-air} \quad (14)$$

P_{V-air} can be calculated from (8). The copper loss characteristic of a magnetic-core inductor for the example specifications built in N40 magnetic material is marked in Fig. 5. In this example, the copper loss of the magnetic-core inductor is much smaller than its core loss (an order of magnitude or more [5]).

C. Q_L Estimation with Given Maximum Inductor Size

In the third step of the design procedure in Fig. 2, we estimate the highest quality factor that can be achieved. If we ignore the copper loss comparing to the core loss of the magnetic-core inductor, the quality factor Q_L can be estimated by (15) and (16):

$$R_{co} \approx \frac{Total\ Core\ Loss}{0.5 I_{pk}^2} = \frac{P_V V}{0.5 I_{pk}^2} \quad (15)$$

$$Q_L \approx \frac{\omega L}{R_{co}} = \omega L \frac{0.5 I_{pk}^2}{P_V V} \quad (16)$$

E.g., for the magnetic-core inductor built in N40, $P_V = 614$ mW/cm^3 at $B_{pk-air} = 1.3$ mT, and $Q_L \approx 198$ by (16). In this example $R_{co} \approx 0.19\ \Omega$ and $R_{cu} \approx 0.03\ \Omega$, where $R_{co} \gg R_{cu}$. Q_L can also be estimated by (2), in which copper loss is included, and $Q_L \approx 171$ by (2).

[5] We note that the simple copper loss calculations of (9) in a cored inductor design may have up to 30% error [22], [24], but this degree of accuracy is sufficient for our present purposes.

D. Size Estimation with Given Minimum Q_L

In this subsection, we illustrate the third step in our inductor design procedure, estimating minimum achievable inductor size for a required quality factor. Because the method introduced in this subsection is not as simple and direct as the method in Section III-B, we begin this subsection with a general description of the method. Then we derive equations needed in our method for inductor size estimation. As we have done in Section III-B, step by step design examples are given to aid understanding of the method.

We again begin with a coreless inductor design, calculate its size and compare the size of a magnetic-core inductor with it. In our method, we define the scaling factor λ as the dimension ratio of a magnetic-core inductor and the coreless inductor for given L, Q_L, f_s and I_{pk}, and we assume that the relative ratio of the 3 dimensions is kept constant during the scaling. Thus, we scale each dimension (x, y, z) describing the shape of the coreless inductor by a factor λ to get the corresponding dimension of a magnetic-core inductor: the coreless inductor thus has $\lambda = 1$, and the magnetic-core inductor with the minimum λ has the smallest size.

Our method has four main steps:

1) Given L, I_{pk}, f_s and minimum required Q_L, design a coreless inductor and get its dimension parameters d_o, d_i, h.
2) Calculate B_{pk-air} of the coreless inductor, compare its P_{V-air} to P_V of other magnetic materials at B_{pk-air} on the graph of P_V vs. $\mu_r^{-0.5}B_{pk}$ and decide the possible best materials for the inductor design.
3) Calculate the scaling factor λ for the possible best materials.
4) Check the flux density B'_{pk}, core loss $P_{V'}$, and copper loss $P_{V'-cu}$ of the magnetic-core inductor after scaling on the graph of P_V vs. $\mu_r^{-0.5}B_{pk}$.

1) Step I, Calculate Coreless Design: From (4), the quality factor Q_L of a coreless inductor can be calculated by (17):

$$Q_L = \frac{\omega L}{R_{cu-air}} = \frac{\mu_0 f_s}{R_{cu-single-turn}} h \ln\left(\frac{d_o}{d_i}\right) \tag{17}$$

$R_{cu-single-turn}$ can be estimated by (9) or (11).

If we assume $d_i = 0.5d_o$, we can solve the dimension parameters d_o, d_i, h of a coreless inductor from (9)/(11), and (17) for given f_s, Q_L and ratio of h and d_o. In Appendix B, we show that this assumption is very reasonable because letting $d_i = 0.5d_o$ yields an inductor with nearly optimum Q_L and thus the smallest size.

2) Step II, Evaluate Magnetic Materials: After calculating the dimensions of the coreless inductor, its B_{pk-air} and P_{V-air} can be calculated by (5) and (8). P_V at B_{pk-air} of all the magnetic materials can be found from the graph of P_V vs. $\mu_r^{-0.5}B_{pk}$. For example, we consider the design of a coreless inductor with $L = 200$ nH, $I_{pk} = 2$ A, $f_s = 30$ MHz, and $Q_L = 116$. We define this coreless inductor as having $\lambda = 1$. Its dimensions are $d_o = 12.7$ mm, $d_i = 6.3$ mm and $h = 6.3$ mm. The question we seek to answer is: if we build an inductor with magnetic materials, how small it could be while achieving the specified minimum Q_L. We first calculate $B_{pk-air} = 1.3$ mT and $P_{V-air} = 1073$ mW/cm^3 and then find P_V for each magnetic material in Fig. 4. N40 is the only magnetic material which has P_V smaller than P_{V-air}, thus the magnetic-core inductor made in N40 is the only possible design with the size smaller than the coreless inductor ($\lambda < 1$) at the same Q_L. Magnetic-core inductors made by other materials will have larger sizes than the coreless inductor and are not considered here. This conclusion is further proved in (26). Just as in Section III-B, we can see here our method in this subsection again helps us to exclude many available magnetic materials in the pool from the complicated problem of inductor size scaling.

3) Step III, Scaling: Here we introduce how to perform the scaling. Before beginning the derivation, we define the following parameters:

1) V, d_o, d_i, h, N, B_{pk}, P_V, P_{V-cu}, R_{co} and R_{cu} are the volume, outside diameter, inside diameter, height, number of turns, average peak ac flux density, core loss density, copper loss density, equivalent core resistance, and copper resistance of a magnetic-core inductor before scaling - i.e., having the same size as the coreless inductor ($\lambda = 1$).
2) V', d'_o, d'_i, h', N', B'_{pk}, P'_V, $P_{V'-cu}$, R'_{co} and R'_{cu} are the same definitions of the magnetic-core inductor after scaling.
3) V, d_o, d_i, h, N_{air}, B_{pk-air}, P_{V-air} and R_{cu-air} are the similiar definitions of the coreless inductor before scaling ($\lambda = 1$)

From the definition above,

$$\lambda = \frac{d'_o}{d_o} = \frac{d'_i}{d_i} = \frac{h'}{h} \tag{18}$$

$$V' = \lambda^3 V \tag{19}$$

Thus: similar to (6),

$$N' = \sqrt{\frac{2\pi L}{\lambda h \mu_0 \mu_r \ln\left(\frac{\lambda d_o}{\lambda d_i}\right)}} = \lambda^{-0.5} N \tag{20}$$

Similar to (7) and from (20),

$$B'_{pk} = \frac{\mu_0 \mu_r N' I_{pk}}{0.5\pi(d'_i + d'_o)} = \lambda^{-1.5} B_{pk} \tag{21}$$

$$P_{V'} = K B'^{\beta}_{pk} = \lambda^{-1.5\beta} P_V \tag{22}$$

From (9) and (11), we observe that $R_{cu-single-turn}$ is constant during scaling. This is because the effective conductor thickness is the skin depth (invariant to scaling). This results in constant "ohms per square", making the total single-turn resistance invariant to scaling. From (12) and (20),

$$R'_{cu} = N'^2 R_{cu-single-turn} = \lambda^{-1} \mu_r^{-1} R_{cu-air} \tag{23}$$

Similar to (14), and from (19) and (23):

$$P_{V'-cu} = \frac{R'_{cu}}{2V'} I^2_{pk} = \lambda^{-4} \mu_r^{-1} P_{V-air} \tag{24}$$

For constant Q_L, the total loss is the same for both the coreless inductor and the magnetic-core inductor, thus from (19), (22) and (24):

$$P_{V'} V' + P_{V'-cu} V' = P_{V-air} V \tag{25}$$

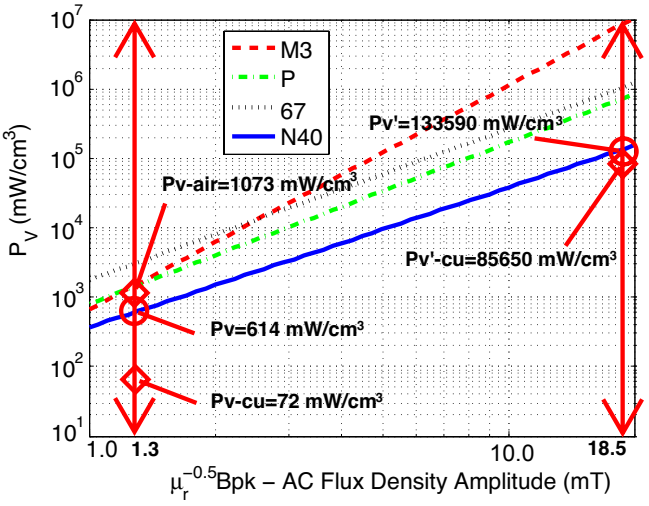

Fig. 6. The magnetic-core inductor after scaling design

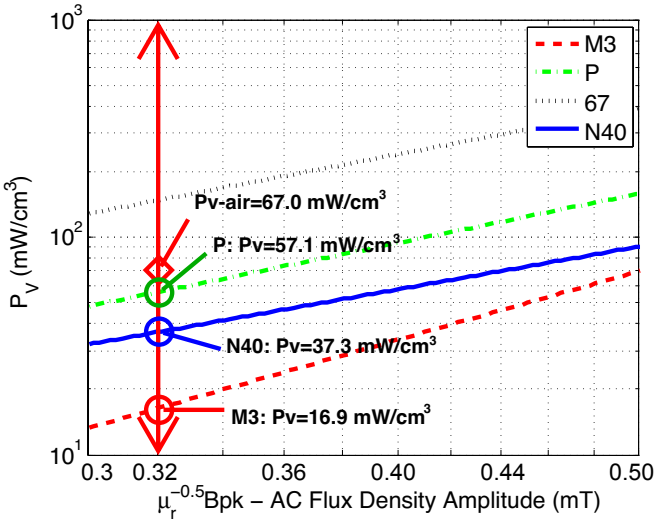

Fig. 7. Loss plots of inductor design scaling example ($d_o = 12.7$ mm, $d_i = 6.3$ mm, $h = 6.3$ mm, $L = 200$ nH, $I_{pk} = 0.5$ A, $f_s = 30$ MHz and $B_{pk-air} = 0.32$ mT).

$$\lambda^{3-1.5\beta}\frac{P_V}{P_{V-air}} + \lambda^{-1}\mu_r^{-1} = 1 \tag{26}$$

The scaling factor λ can be calculated by (26), if we know P_V, relative permeability μ_r, and Steinmetz parameter β of the magnetic material, and P_{V-air} of the coreless inductor. Because of the usual case for Steinmetz parameters (e.g., $\beta > 2$), P_V should be smaller than P_{V-air} to get $\lambda < 1$ from (26). This explains why we don't have to consider magnetic materials which have P_V larger than P_{V-air}. (26) is the key equation for calculating achievable design scaling at constant Q_L through the use of an ungapped magnetic core.

Let's continue our example shown in Fig. 4. For N40 material, $P_V = 614$ mw/cm^3 at $B_{pk-air} = 1.3$ mT, $\beta = 2.02$ at 30 MHz and $\mu_r = 15$, the scaling factor $\lambda = 0.17$ by solving (26).

4) Step IV, Check Design Assumptions: As a last step, we check the flux density B'_{pk}, core loss P'_V, and copper loss $P_{V'-cu}$ of the inductor after scaling on the graph of P_V vs. $\mu_r^{-0.5}B_{pk}$. From (7) and (21):

$$\mu_r^{-0.5}B'_{pk} = \lambda^{-1.5}B_{pk-air} \tag{27}$$

In the example, $P'_V = 1.3 \times 10^5$ mW/cm^3 by (22) and $P'_{V-cu} = 8.6 \times 10^4$ mW/cm^3 by (24) are shown in Fig. 6. We can still see that the core loss dominates the total loss. With completion of this last step, we now have an inductor geometry and scaling that achieves the smallest size at the required Q_L.

5) Inductor Scaling with Multiple choices of Magnetic Materials: Here we give an example of the solution when there is more than one possible material which can be used to build a cored inductor having smaller size than the coreless inductor and thus $\lambda < 1$.

We consider the design of a coreless inductor with $L = 200$ nH, $I_{pk} = 0.5$ A, $f_s = 30$ MHz, and $Q_L = 116$. We design a coreless inductor which has $\lambda = 1$ and dimensions of $d_o = 12.7$ mm, $d_i = 6.3$ mm and $h = 6.3$ mm. We firstly calculate $B_{pk-air} = 0.32$ mT and $P_{V-air} = 67$ mW/cm^3 and then find P_V for each magnetic material in Fig. 7. P, M3 and N40 are magnetic materials which have P_V smaller than P_{V-air}, thus magnetic-core inductors made with these three materials may possibly be smaller than the coreless inductor ($\lambda < 1$). Because P material has both a larger core loss P_V and a larger slope ($= \beta$) of the loss curve than N40 material at B_{pk-air}, we can immediately conclude that P material will not be competitive with N40 material for this design. However, we can't immediately determine which of M3 and N40 materials is better: M3 has a lower P_V at B_{pk-air} but a higher slope of the loss curve than N40. We thus consider both M3 and N40 as possible best materials and calculate their scaling factor λ by (26). We list the calculation results in Table I which also includes P material to confirm our conclusion. From Table I, we can see that the magnetic-core inductor built with N40 still has the smallest scaling factor for the specified minimum Q_L, and represents the best design choice.

TABLE I
COMPARISON OF SCALING FACTOR λ AMONG MAGNETIC-CORE INDUCTORS BUILT WITH P, M3 AND N40 MATERIALS.

Material	P	M3	N40
P_V (mW/cm^3)	57.1	16.9	37.3
μ_r	40	12	15
β	2.33	3.24	2.02
λ by (26)	0.77	0.52	0.16

We check the flux density B'_{pk}, core loss P'_V, and copper loss $P_{V'-cu}$ of the scaled magnetic-core inductor built with N40 material on the graph of P_V vs. $\mu_r^{-0.5}B_{pk}$ by (22), (24) and (27). In the example, the scaled design operates at a normalized flux density $\mu_r^{-0.5}B'_{pk} = 5.0$ mT, $P'_V = 9621$ mW/cm^3, and $P'_{V-cu} = 6819$ mW/cm^3 as illustrated in Fig. 8. We can see that the core loss of N40 is the lowest among the materials at this normalized flux density of the N40 design. If we build a magnetic-core inductor with other materials with the same size after scaling, the inductor will

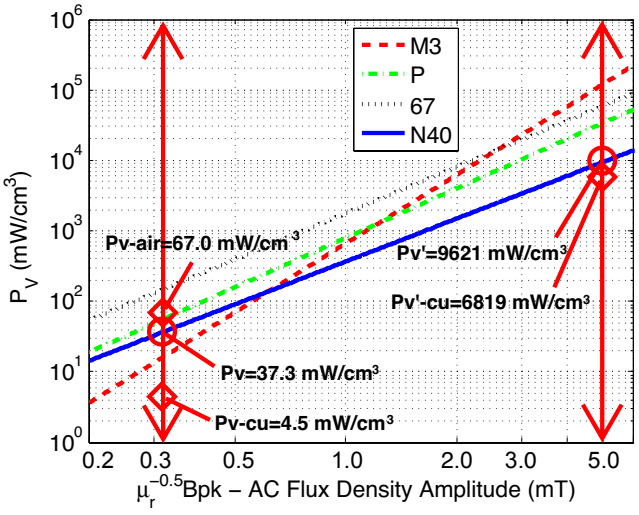

Fig. 8. The magnetic-core inductors after scaling

have a lower quality factor and must have a bigger size to satisfy the design requirement for minimum quality factor; this confirms our conclusion that the magnetic-core inductor built with N40 will have the smallest size.

E. Inductor Design with the Best Magnetic Material

Having satisfied quality factor Q_L and inductor size requirements, the inductor can be designed with the selected best magnetic material (N40). To provide a complete answer for the previous design example, we summarize the results of each step in Fig. 2:

1) We give the design requirements: $L = 200$ nH, $I_{pk} = 2$ A, $f_s = 30$ MHz, minimum $Q_L = 116$ and maximum size of $d_o = 12.7$ mm, $d_i = 6.3$ mm and $h = 6.3$ mm.
2) Given available magnetic materials (67, P, M3 and N40) and their Steinmetz parameters, we determine that N40 is the best material for design.
3) Given the maximum size, estimate the highest Q_L of a magnetic-core inductor with N40 material (about $Q_L = 171$).
4) Given the minimum Q_L, estimate the scaling factor $\lambda = 0.17$ and the minimum size $d_o = 2.2$ mm, $d_i = 1.1$ mm and $h = 1.1$ mm calculated by (18).
5) We check the results in the third and fourth steps and see if they satisfy the design requirements.
6) If we prefer a core inductor with the highest Q_L at the maximum size, the inductor will have a number of turns $N = 4$ calculated by (6), an inductance $L = 199$ nH, and a core size of $d_o = 12.7$ mm, $d_i = 6.3$ mm and $h = 6.3$ mm. Its quality factor Q_L has been estimated in Section III-C as 198 neglecting copper loss and 171 including copper loss. If we prefer a cored inductor with the minimum size at the minimum allowed Q_L of 116, the inductor will have a number of turns $N' = 10$ calculated by (20) and the core size is $d_o = 2.2$ mm, $d_i = 1.1$ mm and $h = 1.1$ mm.

Compared to a coreless design, the magnetic-core inductor with N40 material will have 47% higher quality factor Q_L for the same maximum size or 83% size reduction for the same minimum quality factor.

F. Relationship between Quality Factor Q_L and Inductor Size

The method to calculate the scaling factor λ proposed in Section III-D has two shortcomings: the first is that we may need to rely on some numerical methods to solve the nonlinear equation (26), and the second is that it doesn't reveal the relationship of a magnetic-core inductor's quality factor and its size in a direct and intuitively understandable way. In this subsection, we study the inductor's quality factor as the function of its scaling factor λ.

We again begin our derivations with a coreless inductor. We define quality factor Q_{L0} with given maximum size ($\lambda = 1$) and calculate it by the following equation:

$$Q_{L0} = \frac{\omega L}{R_{cu-air}} = \frac{\mu_0 f}{R_{cu-single-turn}} h \ln\left(\frac{d_o}{d_i}\right) \tag{28}$$

Because $R_{cu-single-turn}$ is constant during the scaling as described before, the quality factor after scaling can be calculated by the following equation:

$$\begin{aligned} Q_L(\lambda) &= \frac{\omega L}{R_{cu}} = \frac{\mu_0 f}{R_{cu-single-turn}} h\lambda \ln\left(\frac{d_o\lambda}{d_i\lambda}\right) \\ &= \lambda Q_{L0} \end{aligned} \tag{29}$$

From (29), we can see there is a linear functional relationship between quality factor Q_L and scaling factor λ for a coreless inductor. This general result for coreless design is well known; see the classic scaling rules for coreless solenoids, for example [1], [41]–[44]. For a magnetic-core inductor, from (23),

$$R'_{cu} = \lambda^{-1}\mu_r^{-1} R_{cu-air} = \frac{\omega L}{\lambda \mu_r Q_0} \tag{30}$$

From (19) and (22),

$$\begin{aligned} R'_{co} &= \frac{P_{V'}V'}{0.5I_{pk}^2} = \frac{\lambda^{3-1.5\beta}P_V V}{0.5I_{pk}^2} = \lambda^{3-1.5\beta}\frac{P_V}{P_{V-air}}\frac{P_{V-air}V}{0.5I_{pk}^2} \\ &= \lambda^{3-1.5\beta}\frac{P_V}{P_{V-air}}R_{cu-air} = \lambda^{3-1.5\beta}\frac{P_V}{P_{V-air}}\frac{\omega L}{Q_{L0}} \end{aligned} \tag{31}$$

From (30) and (31),

$$Q_L(\lambda) = \frac{\omega L}{R'_{cu} + R'_{co}} = \frac{Q_{L0}}{\frac{1}{\lambda\mu_r} + \lambda^{3-1.5\beta}\frac{P_V}{P_{V-air}}} \tag{32}$$

Starting from a baseline design, from (29) and (32), we can plot Q_L vs. λ for magnetic-core inductors made in all available magnetic materials, as well as for a coreless inductor. An example is shown in Fig. 9. The baseline design specifications are $L = 200$ nH, $I_{pk} = 2$ A, $f = 30$ MHz, and $Q_L = 116$. At $\lambda = 1$, the coreless inductor has dimensions $d_o = 12.7$ mm, $d_i = 6.3$ mm and $h = 6.3$ mm. For a given Q_L, we can use results such as in Fig. 9 to find its scaling factor λ and further decide the inductor size for every magnetic material using (18). Moreover, for a given size (scaling factor λ), we can find the quality factor Q_L that is achievable for each material.

While this approach to explore inductor scaling and sizing is informative, it still has some shortcomings. The first one

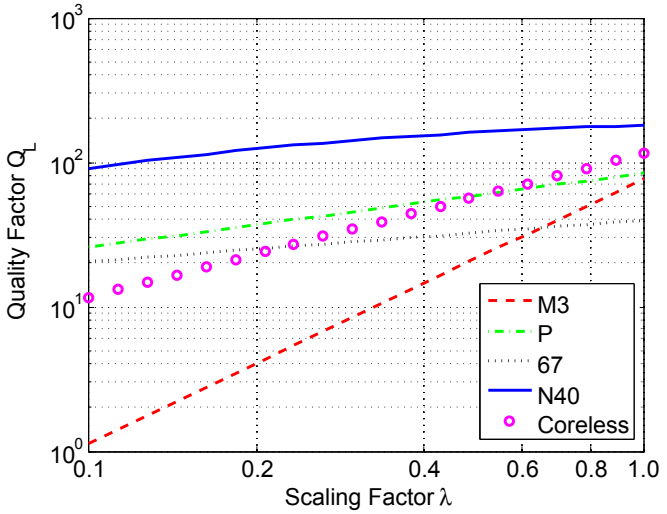

Fig. 9. Q_L vs. λ for coreless inductor and magnetic-core inductors in different mangetic materials ($L = 200$ nH, $I_{pk} = 2$ A and $f = 30$ MHz). At $\lambda = 1$, the coreless inductor has the dimensions $d_o = 12.7$ mm, $d_i = 6.3$ mm and $h = 6.3$ mm.

is that we have to generate a new graph by (29) and (32) for each baseline design of interest. The second one is that we can't a priori exclude some magnetic materials from consideration as we did in Section III-D. If we have dozens of magnetic materials, the graph of Q_L vs. λ will become very complicated. The third one is that all these materials are compared on the graph at a fixed current level and not over a wide operating range. Nevertheless the methods illustrated here provide a better view into design tradeoffs than one otherwise available.

IV. Experimental Verification

We carried out several experiments to verify the design procedure illustrated in this paper. Firstly, we want to verify the design steps 2 and 3 in Fig. 2. That is, given available magnetic materials and design requirements (inductance L, current amplitude I_{pk}, and frequency f_s), we want to determine the best material to yield maximum quality factor Q_L for a given size, and estimate the highest Q_L that can be achieved at that size. Design parameters for the example application are repeated here: $d_o = 12.7$ mm, $d_i = 6.3$ mm, $h = 6.3$ mm, $L = 200$ nH, $I_{pk} = 2$ A, and $f_s = 30$ MHz. As predicted in our design procedure, N40 is the best material and the magnetic-core inductor with N40 has quality factor $Q_L = 171$. We designed and fabricated a magnetic-core inductor with copper foil and N40 core to satisfy the design specifications, and measured its inductance and quality factor with the experimental methods in [22]. To make comparisons with other designs, we fabricated a coreless inductor and magnetic-core inductors with 67, M3 and P materials and similar core sizes. The results are listed and compared in Table II. The cores in M3 and P materials have d_i larger than the design specification, e.g. $\frac{d_i}{d_o} = 0.62$ vs. 0.50. The core loss estimation error due to this is small loss less than 4% higher as shown in Fig. 11 in Appendix B. The core in 67 material has a d_i larger and h lower than the design specifications, and its volume is thus 71.4% of the specified one. The core loss estimation error due to this is only 3.1% higher calculated by (48) where $\beta = 2.18$ [22]. We can see the measurement results fit very well with the predicted values and the magnetic-core inductor with N40 material is the best design compared to others as we have predicted in our design procedure. To some extent, these results also verify the results of approximation and optimizations shown in Appendices A and B.

TABLE II
Comparison among coreless inductors and magnetic-core inductors designed at $I_{pk} = 2$ A and $f_s = 30$ MHz in different magnetic materials.

Material	N40	M3	P	67	Coreless
Suppliers	Ceramic Magnetics	National Magnetics Group	Ferronics	Fairrite	N/A
Permeability	15	12	40	40	1
Designations	T5025-25T	998	11-250-P	59670-00301	N/A
d_o (mm)	12.7	12.7	12.7	12.7	12.7
d_i (mm)	6.3	7.9	7.9	7.2	6.3
h (mm)	6.3	6.4	6.4	5.0	6.3
Turns Number N	4	5	3	3	14
Predicted L (nH)	199	180	219	203	173
Measured L (nH)	230	181	262	235	245
Predicted Q_L	171	74	81	39	116
Measured Q_L	167	65	87	45	96

Secondly, we verified the design step 4 illustrated in Section III-D. That is, given L, I_{pk}, f_s and the minimum Q_L, determine the best material for design and estimate the minimum size achievable for that Q_L requirement. This experiment is much more difficult than the first one because limited availability of core sizes. If we design a magnetic-core inductor with N40 material which has the scaling factor $\lambda = 0.17$ as calculated in Section III-D, the inductor after scaling has 10 turns and dimensions $d'_o = 2.16$ mm, $d'_i = 1.07$ mm and $h' = 1.07$ mm. The winding of copper foil has a width of less than 0.34 mm! It is very hard to wind such a narrow copper foil on this tiny core by hand. The magnetic-core inductor with P material in Section III-D5 has a higher scaling factor λ and thus a larger core size after scaling. So for simplicity, we verified the design of P material instead of N40. The design parameters are repeated here: $L = 200$ nH, $I_{pk} = 0.5$ A, $f_s = 30$ MHz and $Q_L = 116$. The scaling factor $\lambda = 0.77$ calculated by (26) and shown in Table I. The core dimensions after scaling are $d'_o = 9.78$ mm, $d'_i = 4.85$ mm and $h' = 4.85$ mm. The available core with the closest size has dimensions $d'_o = 9.63$ mm, $d'_i = 4.66$ mm and $h' = 3.21$ mm. We designed and fabricated a 3-turn magnetic-core inductor with P material and measured its inductance L and quality factor Q_L. The results are shown in Table III. We can see the measurement results fit very well with the predicted value (for the actual size) and (26) is thus verified.

Thirdly, we verified (32) and the relationship of Q_L vs. λ shown in Fig. 9. The design parameters are repeated here: $L = 200$ nH, $I_{pk} = 2$ A and $f_s = 30$ MHz. At $\lambda = 1$, the coreless inductor has the dimensions $d_o = 12.7$ mm, $d_i = 6.3$ mm

TABLE III
MAGNETIC-CORE INDUCTOR DESIGNED AT $L = 200$ NH, $I_{pk} = 0.5$ A AND $f_s = 30$ MHZ WITH THE SCALING FACTOR $\lambda = 0.77$.

Material	P	Designation	11-220-P
Turns Number N	3	d_o' (mm)	9.63
d_i' (mm)	4.66	h' (mm)	3.21
Predicted L (nH)	168	Measured L (nH)	181
Predicted Q_L	110	Measured Q_L	105

and $h = 6.3$ mm. We design a magnetic-core inductor with N40 material and scaling factor $\lambda = 0.5$. The magnetic-core inductor after scaling thus has dimensions $d_o' = 6.35$ mm, $d_i' = 3.15$ mm and $h' = 3.15$ mm. The closest available core size has the dimensions $d_o' = 5.84$ mm, $d_i' = 3.05$ mm and $h' = 4.06$ mm. We designed and fabricated a 5-turn magnetic-core inductor with N40 materials and measure its inductance L and inductor quality factor Q_L. The results are shown in Table IV. We can see the measurement results fit very well with predicted value (for the actual size) and thus (26) and Fig. 9 are verified.

TABLE IV
MAGNETIC-CORE INDUCTOR DESIGNED AT $L = 200$ NH, $I_{pk} = 2$ A AND $f_s = 30$ MHZ WITH THE SCALING FACTOR $\lambda = 0.5$.

Material	N40	Designation	T231216T
Turns Number N	5	d_o' (mm)	5.84
d_i' (mm)	3.05	h' (mm)	4.06
Predicted L (nH)	198	Measured L (nH)	180
Predicted Q_L	160	Measured Q_L	154

V. CONCLUSION

In this paper, we propose an inductor design procedure using low permeability magnetic materials. The design procedure is based on the use of Steinmetz parameters and low-permeability ungapped cores. With this procedure, different magnetic materials are compared fairly and fast, and both the quality factor Q_L and the size of a magnetic-core inductor can be predicted before the final design. We also compare a magnetic-core inductor design to a coreless inductor design in our design procedure. Some problems, such as optimization of magnetic-core inductors, are also investigated in this paper. The procedure and methods proposed in this paper can help to design magnetic-core inductors with low-permeability rf core materials.

APPENDIX A
APPROXIMATIONS USED IN THE PROPOSED METHODS

In Section III, we average the flux density inside a toroidal core to simplify our calculations. Because the flux density inside a toroidal core is actually not uniform, we need to know if our approximation is reasonable. For a magnetic-core inductor, the average flux density is:

$$B_{pk} = \frac{\mu_0\mu_r N I_{pk}}{0.5\pi(d_o+d_i)} = \frac{I_{pk}}{0.25(d_o+d_i)}\sqrt{\frac{\mu_0\mu_r L}{2\pi h \ln\left(\frac{d_o}{d_i}\right)}} \quad (33)$$

The average total core loss:

$$P(d_i) = P_V V = K B_{pk}^{\beta}\pi\left[\left(\frac{d_o}{2}\right)^2 - \left(\frac{d_i}{2}\right)^2\right]h = \pi h K\left[\frac{I_{pk}}{0.25(d_o+d_i)}\sqrt{\frac{\mu_0\mu_r L}{2\pi h\ln\left(\frac{d_o}{d_i}\right)}}\right]^{\beta}\left[\left(\frac{d_o}{2}\right)^2 - \left(\frac{d_i}{2}\right)^2\right] \quad (34)$$

The total core loss P_0 is calculated without the approximation of uniform flux. From (6),

$$B_{pk}(r) = \frac{\mu_0\mu_r N I_{pk}}{2\pi r} = \frac{I_{pk}}{r}\sqrt{\frac{\mu_0\mu_r L}{2\pi h\ln\left(\frac{d_o}{d_i}\right)}} \quad (35)$$

Where r specifies a radius from the center of the core ($\frac{d_i}{2} < r < \frac{d_o}{2}$).

$$P_0(d_i) = \int_{\frac{d_i}{2}}^{\frac{d_o}{2}} P_V \mathrm{d}V = \int_{\frac{d_i}{2}}^{\frac{d_o}{2}} K B_{pk}(r)^{\beta} 2\pi r h \mathrm{d}r = 2\pi h K\left[I_{pk}\sqrt{\frac{\mu_0\mu_r L}{2\pi h\ln\left(\frac{d_o}{d_i}\right)}}\right]^{\beta}\int_{\frac{d_i}{2}}^{\frac{d_o}{2}} r^{1-\beta}\mathrm{d}r \quad (36)$$

If $\beta \neq 2$,

$$P_0(d_i) = \frac{2\pi h K}{2-\beta}\left[I_{pk}\sqrt{\frac{\mu_0\mu_r L}{2\pi h\ln\left(\frac{d_o}{d_i}\right)}}\right]^{\beta}\left[\left(\frac{d_o}{2}\right)^{2-\beta} - \left(\frac{d_i}{2}\right)^{2-\beta}\right] \quad (37)$$

If $\beta = 2$,

$$P_0(d_i) = \mu_0\mu_r K L I_{pk}^2 \quad (38)$$

We compare P_0 and P and define the error by the following equation:

$$Error = 1 - \frac{P(d_i)}{P_0(d_i)} \quad (39)$$

from (34) and (37), if $\beta \neq 2$,

$$Error = 1 - (2-\beta)2^{\beta-1}\frac{\left[1-\left(\frac{d_i}{d_o}\right)^2\right]\left(1+\frac{d_i}{d_o}\right)^{-\beta}}{1-\left(\frac{d_i}{d_o}\right)^{2-\beta}} \quad (40)$$

from (34) and (38), if $\beta = 2$,

$$Error = 1 - 2\frac{1-\left(\frac{d_i}{d_o}\right)^2}{\left(1+\frac{d_i}{d_o}\right)^2\ln\left(\frac{d_o}{d_i}\right)} \quad (41)$$

We can see $Error$ only depends on the magnetic material Steinmetz parameter β and the dimension ratio of d_i to d_o. $Error$ is plotted in Fig. 10 for different $\frac{d_i}{d_o}$ and β. We can see it is below 10% if β is less than 3 and $\frac{d_i}{d_o} > 0.52$ which is typical for most of available commercial magnetic cores. We assume an optimum $d_i \approx 0.5 d_o$ later. So the error of this approximation should be lower than 10%, which is reasonable.

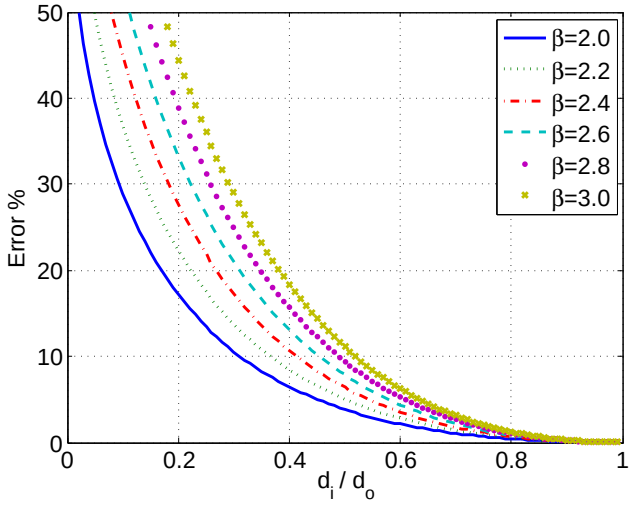

Fig. 10. The error of average flux density approximation.

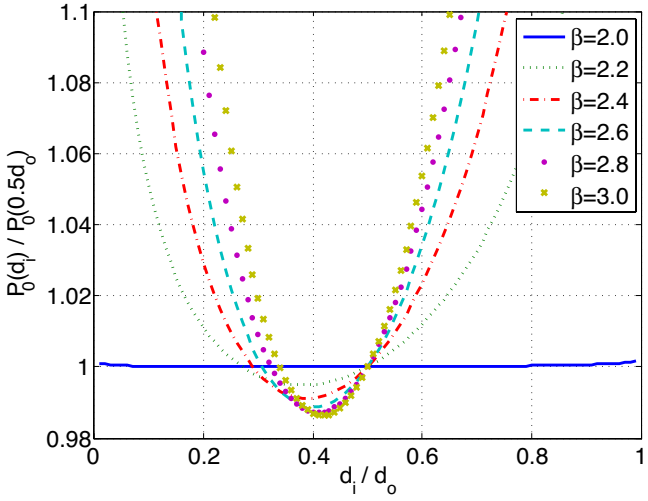

Fig. 11. Plot of core power loss dissipation in a rectangular cross-section toroidal core as a function of $\frac{d_i}{d_o}$, normalized to that with $\frac{d_i}{d_o} = 0.5$. Results are parameterized in Steinmetz parameter β. It can be seen that over a wide range of β, $\frac{d_i}{d_o} = 0.5$ is very close to the optimum, and that results are not highly sensitive to $\frac{d_o}{d_i}$.

APPENDIX B
OPTIMIZATION OF MAGNETIC-CORE INDUCTORS

In Section III, different magnetic materials are compared and evaluated with the assumption that optimum magnetic-core inductors made in all these materials will have the same relative dimensions as the coreless design on which they are based. However, magnetic-core inductors may have their own relative optimum dimensions for the maximum quality factor Q_L or the minimum size for different materials, thus the methods proposed in Section III may not be a fair comparison. That is, we need to establish whether or not the best *shape* for an inductor changes significantly with scale or material characteristics.

As will be seen, the results are quite reasonable and the approaches of Section III lead to near optimum designs under a wide range of conditions. We consider two optimization cases in this paper. First, we assume that a toroidal magnetic-core inductor's d_o and h are restricted to be constant (e.g., as stipulated by the specification of a power electronics circuit), and we optimize d_i to get the maximum quality factor Q_L. Second, we assume its volume V is restricted to be constant, and we optimize d_o, d_i and h to get the maximum quality factor Q_L. In all the optimizations, make the assumption that core losses dominate and neglect copper loss. We do take into account the fact that the flux density inside the core is not uniform when calculating core loss.

A. Optimization of d_i at Fixed d_o and h

From (37) and (38), let $d_i = 0.5d_o$ and we normalize the total core loss $P_0(d_i)$ by the total loss P_0 at $d_i = 0.5d_o$. If $\beta \neq 2$,

$$\frac{P_0(d_i)}{P_0(0.5d_o)} = \left[\frac{\ln 2}{\ln\left(\frac{d_o}{d_i}\right)}\right]^{0.5\beta}\left[\frac{1-\left(\frac{d_i}{d_o}\right)^{2-\beta}}{1-0.5^{2-\beta}}\right] \tag{42}$$

If $\beta = 2$,

$$\frac{P_0(d_i)}{P_0(0.5d_o)} = 1 \tag{43}$$

In (42), $\frac{P_0(d_i)}{P_0(0.5d_o)}$ only depends on the ratio of $\frac{d_o}{d_i}$ and Steinmetz parameter β. We plot P_0 as a function of $\frac{d_o}{d_i}$ for different β in Fig. 11. From Fig. 11, we can see that the optimum d_i is around $0.4d_o$, with an exact value that depends on β. When d_i varies between $0.22d_o$ and $0.64d_o$, the total core loss P is very flat and the deviation from the minimum core loss is less than 10%. We choose $d_i = 0.5d_o$ instead of $d_i = 0.4d_o$ for the following considerations: firstly, $d_i = 0.5d_o$ is a more typical dimension ratio for commercial magnetic cores (e.g., see Table II); secondly, as shown in Appendix A, the error due to the assumption of average flux density is less than 10% if $d_i \geq 0.5d_o$. The error in assuming that the optimum inside diameter is $d_i = 0.5d_o$ is lower than 2% for a wide range of β values. So we can think $d_i = 0.5d_o$ as the nearly-optimum dimension for a wide range of magnetic materials. We can thus compare and evaluate different magnetic materials under the same dimensions and our assumption in Section III is correct.

B. For a Constant Volume V, Optimization of Dimensions d_o, d_i and h

In (38), if $\beta = 2$, core loss P is constant, independent of dimensions, If $\beta \neq 2$, similar to (37),

$$P(h, d_o, d_i) = \frac{2\pi hK}{2-\beta}\left[I_{pk}\sqrt{\frac{\mu_0\mu_r L}{2\pi h \ln\left(\frac{d_o}{d_i}\right)}}\right]^{\beta}\left[\left(\frac{d_o}{2}\right)^{2-\beta} - \left(\frac{d_i}{2}\right)^{2-\beta}\right] \tag{44}$$

$$h = \frac{4V}{\pi\left(d_o^2 - d_i^2\right)} \tag{45}$$

Eliminating h, we find:

$$P(V,d_o,d_i) = \frac{8KV}{(2-\beta)(d_o^2-d_i^2)}\left[I_{pk}\sqrt{\frac{\mu_0\mu_r L(d_o^2-d_i^2)}{8V\ln\left(\frac{d_o}{d_i}\right)}}\right]^{\beta} \left[\left(\frac{d_o}{2}\right)^{2-\beta}-\left(\frac{d_i}{2}\right)^{2-\beta}\right] \quad (46)$$

$$P\left(V,\frac{d_o}{d_i}\right) = \frac{8KV}{2-\beta}\left(I_{pk}\sqrt{\frac{\mu_0\mu_r L}{2V}}\right)^{\beta}\left[\sqrt{\frac{1-\left(\frac{d_i}{d_o}\right)^2}{\ln\left(\frac{d_o}{d_i}\right)}}\right]^{\beta} \left[\frac{1-\left(\frac{d_i}{d_o}\right)^{2-\beta}}{1-\left(\frac{d_i}{d_o}\right)^2}\right] \quad (47)$$

From (47), we know the total loss P only depends on the volume V and the ratio of d_i and d_o. If $\frac{d_i}{d_o}$ constant, we can get:

$$P\left(V,\frac{d_i}{d_o}\right) \propto V^{1-0.5\beta} \quad (48)$$

Because $\beta \geq 2$ in most materials, the total core loss P decreases as the inductor's volume V is increased. Larger volume will always help reduce core loss and improve quality factor Q_L in a magnetic-core inductor (so long as core loss is dominant).

If we normalize P by $P(d_i = 0.5d_o)$:

$$P(V,0.5) = \frac{2KV}{2-\beta}\left(I_{pk}\sqrt{\frac{\mu_0\mu_r L}{2V}}\right)^{\beta}\left[\sqrt{\frac{1-2^{-2}}{\ln(2)}}\right]^{\beta} \left[\frac{1-2^{\beta-2}}{1-2^{-2}}\right] \approx \frac{2KV}{2-\beta}\left(I_{pk}\sqrt{\frac{\mu_0\mu_r L}{2V}}\right)^{\beta}\left[\frac{1-2^{\beta-2}}{0.75}\right] \quad (49)$$

For a constant volume V,

$$\frac{P\left(V,\frac{d_i}{d_o}\right)}{P(V,0.5)} = \left[\sqrt{\frac{1-\left(\frac{d_i}{d_o}\right)^2}{\ln\left(\frac{d_o}{d_i}\right)}}\right]^{\beta}\left[\frac{1-\left(\frac{d_i}{d_o}\right)^{2-\beta}}{1-\left(\frac{d_i}{d_o}\right)^2}\right] \left[\frac{0.75}{1-2^{\beta-2}}\right] \quad (50)$$

Notice that in (50) the normalized P only depends on the material's Steinmetz parameter β and the ratio of d_i to d_o, independent of V and other individual dimension parameters (e.g., d_o, d_i, or h). Fig. 12 plots the normalized P vs. $\frac{d_i}{d_o}$. For $d_i > 0.3d_o$, the total loss P is flat and almost constant. Thus we can conclude that, to a first approximation, the total loss P only depends on the inductor's volume V, and is independent of its dimensions d_i, d_o, and h when $d_i > 0.3d_o$. In other words, for a given total core loss P, there is only one solution for the volume V that will achieve it, but there are many solutions for the dimensions d_i, d_o, and h that can be used. Moreover, from this result we can conclude that we needn't concern ourselves with the optimum geometry changing with absolute scale (in terms of core loss), so may confidently use the results of Section III in finding an optimum inductor design.

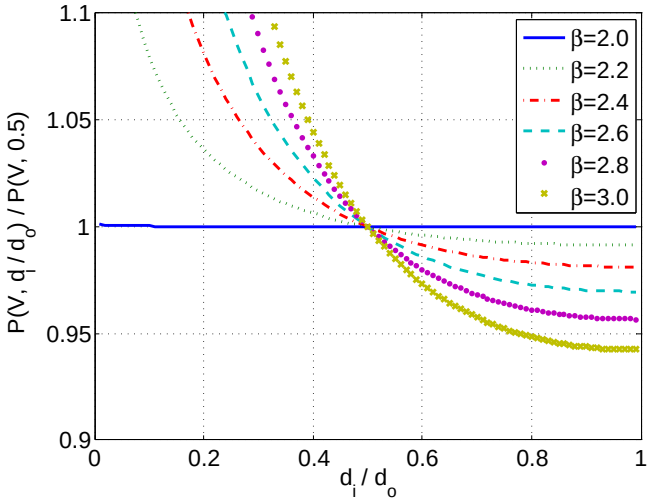

Fig. 12. Core loss optimization for a constant volume.

REFERENCES

[1] D. Perreault, J. Hu, J. Rivas, Y. Han, O. Leitermann, R. Pilawa-Podgurski, A. Sagneri, and C. Sullivan, "Opportunities and challenges in very high frequency power conversion," *24th Annu. IEEE Applied Power Electronics Conf. and Expo.*, pp. 1–14, Feb. 2009.

[2] J. Rivas, "Radio frequency dc-dc power conversion," Ph.D. dissertation, Massachusetts Institute of Technology, Sep. 2006.

[3] J. Rivas, Y. Han, O. Leitermann, A. Sagneri, and D. Perreault, "A high-frequency resonant inverter topology with low-voltage stress," *IEEE Trans. Power Electron.*, vol. 23, no. 4, pp. 1759–1771, Jul. 2008.

[4] D. Hamill, "Class DE inverters and rectifiers for dc-dc conversion," *27th IEEE Power Electronics Specialists Conf.*, vol. 1, pp. 854–860, Jun. 1996.

[5] N. Sokal and A. Sokal, "Class E-A new class of high-efficiency tuned single-ended switching power amplifiers," *IEEE J. Solid-State Circuits*, vol. 10, no. 3, pp. 168–176, Jun. 1975.

[6] N. Sokal, "Class-E rf power amplifiers," *QEX*, pp. 9–20, Jan./Feb. 2001.

[7] R. Frey, "High voltage, high efficiency MOSFET rf amplifiers - design procedure and examples," Advanced Power Technology, Application Note APT0001, 2000.

[8] ——, "A push-pull 300-watt amplifier for 81.36 MHz," Advanced Power Technology, Application Note APT9801, 1998.

[9] ——, "500w, class E 27.12 MHz amplifier using a single plastic MOSFET," Advanced Power Technology, Application Note APT9903, 1999.

[10] M. Iwadare and S. Mori, "Even harmonic resonant class E tuned power amplifer without rf choke," *Electron. and Commun. in Japan (Part I: Commun.)*, vol. 79, no. 2, pp. 23–30, Jan. 1996.

[11] S. Kee, I. Aoki, A. Hajimiri, and D. Rutledge, "The class-E/F family of ZVS switching amplifiers," *IEEE Trans. Microw. Theory Tech.*, vol. 51, no. 6, pp. 1677–1690, Jun. 2003.

[12] A. Sagneri, "Design of a very high frequency dc-dc boost converter," Master's thesis, Massachusetts Institute of Technology, Feb. 2007.

[13] W. Bowman, F. Balicki, F. Dickens, R. Honeycutt, W. Nitz, W. Strauss, W. Suiter, and N. Ziesse, "A resonant dc-to-dc converter operating at 22 Megahertz," *3rd Annu. IEEE Applied Power Electronics Conf. and Expo.*, pp. 3–11, Feb. 1988.

[14] R. Pilawa-Podgurski, A. Sagneri, J. Rivas, D. Anderson, and D. Perreault, "Very-high-frequency resonant boost converters," *IEEE Trans. Power Electron.*, vol. 24, no. 6, pp. 1654–1665, Jun. 2009.

[15] R. Gutmann, "Application of RF circuit design principles to distributed power converters," *IEEE Trans. Ind. Electron. Contr. Instrum.*, vol. 27, no. 3, pp. 156–164, Aug. 1980.

[16] J. Jóźwik and M. Kazimierczuk, "Analysis and design of class-e^2 dc/dc converter," *IEEE Trans. Ind. Electron.*, vol. 37, no. 2, pp. 173–183, Apr. 1990.

[17] S. Ajram and G. Salmer, "Ultrahigh frequency dc-to-dc converters using GaAs power switches," *IEEE Trans. Power Electron.*, vol. 16, no. 5, pp. 594–602, Sep. 2001.
[18] R. Steigerwald, "A comparison of half-bridge resonant converter topologies," *IEEE Trans. Power Electron.*, vol. 3, no. 2, pp. 174–182, Apr. 1988.
[19] R. Redl and N. Sokal, "A 14-MHz 100-watt class E resonant converter: principle, design considerations and measured performance," *17th IEEE Power Electronics Specialists Conf.*, pp. 68–77, 1986.
[20] W. Tabisz and F. Lee, "Zero-voltage-switching multi-resonant technique-a novel approach to improve performance of high frequency quasi-resonant converters," *19th IEEE Power Electronics Specialists Conf.*, pp. 9–17, Apr. 1988.
[21] F. Lee, "High-frequency quasi-resonant converter technologies," *Proceedings of the IEEE*, vol. 76, no. 4, pp. 377–390, Apr. 1988.
[22] Y. Han, G. Cheung, A. Li, C. Sullivan, and D. Perreault, "Evaluation of magnetic materials for very high frequency power applications," *39th IEEE Power Electronics Specialists Conf.*, pp. 4270–4276, Jun. 2008.
[23] Y. Han, "Circuits and passive components for radio-frequency power conversion," Ph.D. dissertation, Massachusetts Institute of Technology, Feb. 2010.
[24] Y. Han, G. Cheung, A. Li, C. Sullivan, and D. Perreault, "Evaluation of magnetic materials for very high frequency power applications," *IEEE Trans. Power Electron.*, vol. 27, no. 1, pp. 425–435, Jan. 2012.
[25] R. Erickson and D. Maksimović, *Fundamentals of Power Electronics*, 2nd ed. Springer Science and Business Media Inc., 2001, ch. 14 and 15.
[26] Y. Han and D. Perreault, "Inductor design methods with low-permeability rf core materials," *IEEE Energy Conversion Congress and Exposition*, pp. 4376–4383, Sep. 2010.
[27] C. Sullivan, W. Li, S. Prabhakaran, and S. Lu, "Design and fabrication of low-loss toroidal air-core inductors," *38th IEEE Power Electronics Specialists Conf.*, pp. 1757–1759, Jun. 2007.
[28] M. Mu, Q. Li, D. Gilham, F. Lee, and K. Ngo, "New core loss measurement method for high frequency magnetic materials," *IEEE Energy Conversion Congress and Exposition*, pp. 4384–4389, Sep. 2010.
[29] W. Roshen, "A practical, accurate and very general core loss model for nonsinusoidal waveforms," *IEEE Trans. Power Electron.*, vol. 22, no. 1, pp. 30–40, Jan. 2007.
[30] J. Li, T. Abdallah, and C. Sullivan, "Improved calculation of core loss with nonsinusoidal waveforms," *36th Annual Meeting of IEEE Industry Applications Society*, vol. 4, pp. 2203–2210, Sep./Oct. 2001.
[31] K. Venkatachalam, C. Sullivan, T. Abdallah, and H. Tacca, "Accurate prediction of ferrite core loss with nonsinusoidal waveforms using only steinmetz parameters," *2002 IEEE Workshop on Computers in Power Electronics*, pp. 36–41, Jun. 2002.
[32] M. Albach, T. Durbaum, and A. Brockmeyer, "Calculating core losses in transformers for arbitrary magnetizing currents a comparison of different approaches," *27th IEEE Power Electronics Specialists Conf.*, vol. 2, pp. 1463–1468, Jun. 1996.
[33] J. Reinert, A. Brockmeyer, and R. D. Doncker, "Calculation of losses in ferro- and ferrimagnetic materials based on the modified steinmetz equation," *IEEE Trans. Ind. Applicat.*, vol. 37, no. 4, pp. 1055–1061, Jul./Aug. 2001.
[34] A. Brockmeyer, "Dimensionierungswekzeug f"ur magnetische bauelemente in stromrichteranwendungen," Ph.D. dissertation, Aachen University of Technology, 1997.
[35] C. Steinmetz, "On the law of hysteresis," *Proc. of the IEEE*, vol. 72, pp. 197–221, Feb. 1984.
[36] R. Erickson and D. Maksimović, *Fundamentals of Power Electronics*, 2nd ed. Springer Science and Business Media Inc., 2001, ch. 13.
[37] S. Mulder, "Power ferrite loss formulas for transformer design," *Power Conversion and Intelligent Motion*, vol. 21, no. 7, pp. 22–31, Jul. 1995.
[38] E. Snelling, *Soft ferrites, properties and applications*, 2nd ed. Butterworths, 1988.
[39] A. Goldberg, "Development of magnetic components for 1-10 MHz dc/dc converters," Ph.D. dissertation, Massachusetts Institute of Technology, Sep. 1988.
[40] A. Goldberg, J. Kassakian, and M. Schlecht, "Issues related to 1-10-MHz transformer design," *IEEE Trans. Power Electron.*, vol. 4, no. 1, pp. 113–123, Jan. 1989.
[41] R. Medhurst, "H.f. resistance and self-capacitance of single-layer solenoids," *Wireless Engineer*, pp. 35–43, Mar. 1947.
[42] ——, "Q of solenoid coils," *Wireless Engineer*, p. 281, Sep. 1947.
[43] M. Callendar, "Q of solenoid coils," *Wireless Engineer (Correspondence)*, p. 185, Jun. 1946.
[44] T. Lee, *Planar Microwave Engineering: A Practical Guide to Theory, Measurement, and Circuits*. Cambridge University Press, 2004, ch. 6.